Terahertz dynamics in the glycerol-water system

Johanna Kölbel [1], Walter Schirmacher [2,3], Evgenyi Shalaev,[4] and J. Axel Zeitler [1,*]

[1]*Department of Chemical Engineering, University of Cambridge, Cambridge CB3 0AS, United Kingdom*
[2]*Department of Physics, Johannes Gutenberg University, 55099 Mainz, Germany*
[3]*Center for Life Nano Science @Sapienza, Istituto Italiano di Tecnologia, 295 Viale Regina Elena, I-00161 Roma, Italy*
[4]*AbbVie, Irvine, California 92612, USA*

The model glass former glycerol and its aqueous mixtures were investigated with terahertz-time-domain spectroscopy (THz-TDS) in the frequency range 0.3–3.0 THz at temperatures from 80 to 305 K. It was shown that the infrared absorption coefficient measured with THz-TDS can be theoretically related to the reduced Raman intensity ($\propto \alpha/\omega^2$) and the reduced density of states ($\propto \alpha/\omega^3$) and the agreement with experimental results confirms this. The data were further used to investigate the behavior of model glasses in the harmonic (below the glass transition temperature T_g), anharmonic (above T_g), and liquid regimes. The onset temperature of molecular relaxation as measured by the infrared active dipoles, T_g, was found to correlate with the onset of anharmonic effects, leading to an apparent shift of the boson peak and obscuring it at elevated temperatures. The influence of clustered and unclustered water on the dynamics, the boson peak, and the vibrational dynamics was also investigated. A change in structural dynamics was observed at a water concentration of approximately 5 wt %, corresponding to a transition from isolated water molecules distributed homogeneously throughout the sample to the presence of small water clusters and an increased number of water-water hydrogen bonds which lower the barriers on the potential energy surface.

I. INTRODUCTION

A. Dynamics of glass formers

Upon cooling of an organic molecular liquid to temperatures below its melting point, it either forms a crystal or remains disordered, ultimately forming an amorphous solid. Initially, at temperatures just below its freezing temperature a liquid is referred to as supercooled. In such thermodynamically metastable systems the Stokes-Einstein relation breaks down, and diffusion and viscosity decouple [1–3]. The molecular arrangement remains similar to that of liquids and long-range order is completely absent.

The liquid-to-glass transition temperature T_g is usually defined as the temperature at which the viscosity acquires a value of about 10^{12} Pa s, associated with a sharp change in the thermal expansion coefficient and specific heat. Approaching the liquid-to-glass transition from above, a number of characteristic changes in the type of the molecular motions occur, which have been described both in terms of mode-coupling theory (MCT) [2,4,5] and in terms of the potential energy surface (PES) [3,6] formed by the configurations of the liquid, which approaches the glassy arrest.

MCT [2,4,5] describes an idealized liquid-to-glass transition, in which a nonergodic state with vanishing molecular mobility is formed. This transition, which occurs at a temperature T_c above the calorimetric glass transition temperature T_g, is associated with two characteristic relaxation processes: (i) (fast) secondary or β relaxation, visualized by the rattling of molecules inside the cage formed by their neighbors, and (ii) primary or α relaxation associated with leaving this cage or, equivalently, by the presence of a finite mobility [4,5]. While both relaxation processes—associated with a characteristic fractal frequency dependence of the spectra—have been widely experimentally verified in glass-forming liquids [7–12], MCT fails to account for activated processes, which occur between T_c and T_g. In this interval the viscosity acquires a very strong temperature dependence, which then eventually leads to the very high value at T_g.

The relaxation in this regime has been discussed in terms of the PES of the glass-forming liquids [3,6,13]: The MCT critical temperature is associated with a change from a saddle-dominated PES towards a minimum-dominated one. The activated relaxation steps then occur between the PES minima. In this regime the α relaxation leads to a characteristic peak in the dielectric spectra [8,9], followed (at higher frequency) by an extended wing or maximum, associated with the slow, activated β relaxation (Johari-Goldstein relaxation [12,14,15]).

Terahertz-time-domain spectroscopy (THz-TDS) probes frequencies in the range of 0.35 to 3 THz by coupling to dipole moments at photon energies on the order of the hydrogen bond strength and picosecond relaxation time. It hence provides

---

*jaz22@cam.ac.uk

a sensitive probe of molecular motions in condensed phase organic molecular materials. Such motions are the described two types of α and β relaxation above T_g and the vibrational motions below T_g. Past studies using THz-TDS have investigated the complex interplay between reorientation motion and vibration dynamics in hydrogen-bonded liquids [16–18].

Poley was the first to suggest the existence of an additional region of dipolar absorption at terahertz frequencies in liquids [19,20]. By using more advanced spectroscopic techniques it was later possible to observe this experimentally and hence the term *Poley absorption* is sometimes used when referring more generically to absorption in the terahertz range.

Due to the inherent disorder of glasses, at low frequency, no discrete phonon modes can be sustained. Instead, in Raman spectra, and in the reduced terahertz absorption spectra (divided by the squared frequency), a featureless peak has been observed, which has been called the boson peak (BP), because it exhibits the temperature and frequency dependence of the Bose occupation function $n(\omega) = [\exp(\hbar\omega/k_BT) - 1]^{-1}$. This, in turn, implies that the vibrational spectrum is temperature independent and, consequently, of harmonic origin.

The boson peak is observed also in the vibrational spectra of glasses as an excess over the Debye vibrational density of states (VDOS) $g_D(\omega) \propto \omega^2$, or, equivalently, as a peak in the reduced VDOS $g(\omega)/\omega^2$ by inelastic neutron [21,22], x-ray [23], and nuclear scattering [24]. Because the frequency dependence of the VDOS is reflected in the temperature dependence of the specific heat, the reduced specific heat $C(T)/T^3$ of glasses exhibits a broad maximum near 10 K, which, accordingly, is also called the boson peak.

The BP has been found in a variety of glasses [25], as well as disordered crystals [26]. A lively discussion surrounds its origin. While heterogeneous-elasticity theory, based on the model assumption of spatially fluctuating elastic moduli [27–30], gives good agreement to experimental and simulational data of glasses with central-atomic forces, evidence has been proposed that the BP in network glasses is due to a washed-out van Hove singularity [24,31–33]. Alternatively, also the presence of local modes due to soft potentials has been proposed as an origin of the BP [34,35], which are supposed to hybridize with the wavelike modes [35–37].

Within the PES picture the disorder-related harmonic motions are thought to occur in deep minima of the landscape [3,6]. At higher temperatures, first anharmonic phenomena occur at T^*, which give rise to temperature-dependent parts of the VDOS. In our paper we call the onset of anharmonic or relaxational motions "onset of mobility" for short. As temperature increases further, a smooth crossover appears from anharmonic vibrations to secondary relaxation at T_g^*, and then to primary relaxations in the liquid state. It is important to emphasize that the calorimetric glass transition temperature, T_g, is not identical to the T_g^* as measured by terahertz spectroscopy, but that they frequently coincide.

Glycerol is a widely studied network material and model system for a glass former as it is nontoxic and easily supercools and has been investigated with experimental techniques like Raman scattering [38,39], infrared spectroscopy [40,41], dielectric spectroscopy [8–11,42,43], neutron and light scattering [22,44,45], differential scanning calorimetry (DSC) [46], and terahertz spectroscopy

[47], as well as theoretical work with molecular dynamics simulations [40,48]. Its calorimetric T_g was found to lie between 185 and 194 K [9,46,49,50]. In glycerol, the VDOS extends up to 7 THz [9,22,24,25].

Glycerol is hence a promising model system to investigate whether anharmonic effects can be detected at temperatures even below T_g^*. Here we study the impact of temperature changes on glycerol dynamics, especially anharmonic effects that can obscure the BP.

The density of states of pure glycerol, including the elevated temperature range, where the spectrum becomes temperature dependent, is well documented: Chumakov *et al.* [24] embedded a probe molecule in a glass matrix and monitored its translational motions with nuclear inelastic scattering. Because the probe followed the collective motions of the glass with a correlation length larger than the probe size, the density of states of collective motions of the glass matrix, i.e., the VDOS multiplied with the Debye-Waller factor, was directly measured. It was reported that a significant part of the BP in the model glass former glycerol is constituted of collective modes and that it disappears close to T_g due to increased sample mobility. They further observed an exponential decrease in the reduced VDOS at energies above the BP maximum [24].

Wuttke *et al.* found that the reduced density of states of glycerol is temperature independent at frequencies above the BP maximum [51]. At frequencies below the maximum, a temperature-dependent change was observed even at temperatures below T_g. These temperature-dependent changes in the BP occur above the characteristic temperature T^*, which coincides with the onset of limited mobility and anharmonicity. This onset at T^* is typically too subtle to be detected in DSC measurements [52]. Ruggiero *et al.* described T^* in terms of the Johari-Goldstein β-relaxation process, also called $T_{g,\beta}$ [53].

B. Glycerol-water mixtures

Modern biopharmaceutical drugs are often developed into complex amorphous formulations that are prepared by spray drying or freeze drying (lyophilization). Given its resistance to crystallization, glycerol is used widely as a so-called cryoprotectant of cells and organs and also to stabilize lyophilized proteins [54,55]. Some pharmaceutical degradation mechanisms are catalyzed by water clusters and the influence of water content on the stability of lyophilized products has been investigated previously [56]. In macromolecules, water can both serve to stabilize the native structure while simultaneously acting as a catalyst for destabilization. Starciuc *et al.* suggested that unclustered water molecules (that are commonly found in products containing only a few wt % water) are less catalytically active than water clusters [57]. They hypothesized that proton transfer becomes possible only once a water-clustering threshold is exceeded, thereby supporting pharmaceutical degradation reactions such as amide hydrolysis and deamidation.

The model system of glycerol-water mixtures has been studied widely [40,42,58–61]: Towey *et al.* used a combination of neutron diffraction experiments and computational modeling to investigate the structure and hydrogen bonding of pure glycerol [60], dilute aqueous glycerol solution [59],

and glycerol-water mixtures for glycerol mole fractions of $x_g = 0.05, 0.10, 0.25, 0.50, 0.80$, and 1.00 [61]. They found bipercolating clusters of both water and glycerol in samples containing a mole fraction between 0.75 and 0.5 water (i.e., between 16.4 and 37 wt % water). They further found that water maintained its full hydrogen-bonding capacity independently of the glycerol concentration.

Murata and Tanaka found evidence for a water liquid-liquid transition (LLT) without macroscopic phase separation in glycerol-water mixtures containing between approximately 45.5 and 56 wt % water [58].

Recently, Starciuc *et al.* investigated glycerol-water mixtures containing between 0 and 40 wt % water with low- and high-wave-number Raman spectroscopy, and three water-content regions were found [57]. This confirmed the existence of a threshold for water clustering in glycerol. A transition from predominantly unclustered water molecules to small water clusters was reported at 6.1 ± 0.7 wt % water and a second threshold at 18.6 ± 4.4 wt % water, which was proposed to correspond to the formation of large water clusters associated with the onset of freezing.

And while glycerol and glycerol-water systems have been investigated thoroughly with a range of methods, there has not yet been a comprehensive study in the terahertz frequency range over a range of temperatures to investigate the role of water, especially the formation of water clusters, in glycerol-water mixtures with a water content below 30 wt % water, where past studies have shown the existence of several water regions. Typical water content specification limits for freeze-dried pharmaceuticals are below 5 wt %. By understanding the structural dynamics of the glycerol-water system, such water content specifications in the design of pharmaceutical products can be scientifically substantiated and their design can be optimized.

The dynamics of the model system of glycerol-water mixtures are investigated with THz-TDS by varying both the temperature and the water concentration. The aim was to extract as much information as possible about both the glass and the amorphous solid and to investigate the role of the BP and the shape of the VDOS and their relationship with the glass transition temperatures.

In addition to the THz-TDS data at various (cryogenic) temperatures, high-quality room-temperature data of liquid glycerol-water mixtures with different water concentrations were also acquired to further understand how the water content influences the terahertz spectra of the liquids.

II. MATERIALS AND METHODS

A. Variable-temperature THz-TDS measurements

Glycerol was obtained from Sigma Aldrich (Poole, U.K.) and was mixed with Milli-Q water (IQ 7000, Merck, Darmstadt, Germany, resistivity 18.2 MΩ cm) in various ratios (0–30 wt % water). After mixing, the samples were sealed and left standing or briefly degassed inside a desiccator attached to a vacuum pump. No experimental differences between samples prepared by the two methods were observed. For subsequent measurements, a drop of liquid sample was sealed between two z-cut quartz windows (Crystran, U.K.)

separated by a 100-μm-thick PTFE spacer in a liquid cell which was then fit into the cryostat and placed under vacuum. The samples were analyzed in transmission using a commercial Terapulse 4000 spectrometer (TeraView Ltd., Cambridge, U.K.) with a liquid nitrogen cryostat attached, as described by Sibik *et al.* [62]. Two z-cut quartz windows (Crystran, U.K.) were used for reference measurements. The spectral range the instrument was able to access was in the range 0.35–3 THz, depending on sample absorption.

Utilizing the cryostat and liquid nitrogen cooling, a wide range of temperatures was studied (80–305 K). At each temperature, a co-average of 1000 waveforms was acquired for both reference and sample and used to calculate the optical constants as described in the Supplemental Material [63] (see also Refs. [64,65] therein).

To increase reproducibility and facilitate comparison between different water concentrations, the measurements were controlled with a computer program that kept the length of temperature steps and therefore the overall heating rate constant at about 1 K min^{-1}.

B. THz-TDS measurements at room temperature

Glycerol and its mixtures were prepared following the same steps as described above. However, instead of sealing the sample into a liquid cell that fit into the cryostat, a room-temperature liquid cell was utilized which was easier to assemble. This liquid cell also consisted of two z-cut quartz windows separated by a 100-μm-thick PTFE spacer. This was subsequently placed into the measurement chamber which was purged with dry nitrogen and samples were analyzed in transmission using the Terapulse 4000 spectrometer utilizing the same settings as for measurements at variable temperatures.

C. Relationship between reduced density of states measured with THz-TDS, neutron, Raman, and nuclear inelastic scattering

In this section we develop theoretical ideas relating the infrared absorption coefficient $\alpha(\omega)$ to the mechanical degrees of freedom. The absorption coefficient is related to the dielectric loss function by $\alpha(\omega) = \omega \epsilon''(\omega)/(n(\omega)c)$. The loss function, in turn, can be related to the complex shear modulus $G(\omega) = G'(\omega) - iG''(\omega)$ by the formula of Gemant [66–68], as utilized by Schirmacher, Ruocco, and Mazzone [69], where V denotes an activation volume, i.e., the volume of the material region that participates in the relaxation step:

$$\epsilon'' = \text{Im}\left\{\frac{1}{1 + \frac{VG}{kT}}\right\} \propto \text{Im}\left\{\frac{1}{G}\right\}. \quad (1)$$

$G(\omega)$ is the complex mechanical shear modulus, the frequency dependence of which is mainly given by the sound attenuation of the shear waves $\Gamma(\omega)$ [30]:

$$G(\omega) = G'(\omega)[1 - i\Gamma(\omega)/\omega]. \quad (2)$$

Therefore, $\alpha(\omega)$ is given by

$$\alpha(\omega) \propto \omega \epsilon''(\omega) \propto \omega^2 \frac{\Gamma(\omega)}{1 + \Gamma(\omega)^2/\omega^2}. \quad (3)$$

This means that we can extract the transverse sound attenuation coefficient from the infrared absorption, which is usually not accessible to experimental investigation.

A very similar formula can be obtained for the Raman intensity $I_{AB}(\omega) = [n(\omega) + 1]\chi''_{AB}(\omega)$, where A and B denote V or H polarization. The Raman susceptibilities can be written as [29]

$$\chi''_{VV}(\omega) = \frac{4}{3}\chi''_{VH}(\omega) + Af_1\chi^{\xi}_{L}(\omega), \qquad (4)$$

$$\chi''_{VH}(\omega) = Af_2\frac{1}{30}\left(2\chi^{\xi}_{L}(\omega) + 3\chi^{\xi}_{T}(\omega)\right), \qquad (5)$$

where

$$\chi^{\xi}_{L,T}(\omega) = \text{Im}\left\{\frac{3}{k_\xi^3}\int_0^{k_\xi} k^2 dk \frac{k^2}{-\omega^2 + k^2 c_{L,T}^2(\omega)}\right\}$$
$$= \text{Im}\left\{\frac{1}{c_{L,T}^2(\omega)} + O(\omega^2)\right\}. \qquad (6)$$

These equations have been derived under the assumption of fluctuating Pockels constants [70,71]. The upper cutoff k_ξ is proportional to the inverse correlation length ξ of the Pockels constant fluctuations. $c_L(\omega)$ and $c_T(\omega)$ are the complex longitudinal and transverse sound velocities. f_1 and f_2 are the prefactors of the longitudinal and transverse Pockels correlation functions, respectively. In terms of the longitudinal modulus $M(\omega)$ and the shear modulus $G(\omega)$, the complex sound velocities are given by

$$\rho c_L^2(\omega) = M(\omega), \quad \rho c_T^2(\omega) = G(\omega), \qquad (7)$$

where ρ is the mass density.

Because the inverse of the transverse sound velocity is much larger than the longitudinal one, the Raman scattering intensity will be dominated by the transverse susceptibility. For low enough frequencies we essentially have

$$I_{AB}(\omega) \propto [n(\omega) + 1]\text{Im}\left\{\frac{1}{G}\right\}. \qquad (8)$$

So we expect the reduced Raman intensity to be proportional to the infrared absorption coefficient divided by ω^2:

$$\tilde{I}(\omega) \equiv \frac{I(\omega)}{\omega(n(\omega) + 1)} \propto \alpha(\omega)/\omega^2. \qquad (9)$$

The reduced Raman intensity is also commonly represented as [71]

$$\tilde{I}(\omega) \propto C(\omega)\frac{g(\omega)}{\omega^2} \qquad (10)$$

with the phenomenological frequency-dependent coupling coefficient $C(\omega)$ and the reduced DOS $\frac{g(\omega)}{\omega^2}$. In most materials $C(\omega) \propto \omega$ [72].

Thus, the reduced DOS $\frac{g(\omega)}{\omega^2}$ is related to the infrared absorption coefficient by

$$\frac{g(\omega)}{\omega^2} \propto \frac{\alpha(\omega)}{\omega^3}. \qquad (11)$$

III. RESULTS AND DISCUSSION

A. Pure glycerol measurements and analysis

1. The Boson peak

The terahertz absorption spectra measured by THz-TDS of the investigated glycerol-water samples are featureless. An example spectrum is shown in Fig. 1(a). Without further analysis it is not possible to distinguish between the glass and the liquid states.

For comparison of the infrared data with neutron and Raman scattering data, the absorption coefficient divided by frequency to the powers of 2 and 3 is plotted in Figs. 1(b) and 1(c), respectively. At low temperatures, the BP is clearly visible at around 1 THz and its amplitude and center frequency are mostly constant. With increasing temperature, the maximum appears to shift to lower frequencies before features of the BP can no longer be detected at even higher temperatures.

Chumakov *et al.* [24] used nuclear inelastic scattering to measure delocalized collective motions in glycerol with a correlation length greater than 20 Å. In comparison to the measurements by Wuttke *et al.* [44] the nuclear inelastic scattering data detect the BP at slightly lower frequency, while exhibiting a similar shape overall [Fig. 1(d)]. In pure glycerol Wuttke *et al.* found a pronounced BP at 170 K that disappeared at 210 K. This observation is confirmed by our THz-TDS measurements [Fig. 1(c)]. Even at very low temperatures (below 120 K), the BP, as measured with THz-TDS, increases in intensity while the maximum frequency stays constant. In the same temperature interval, the neutron data show no temperature-dependent change.

The BP was also visualized with low-frequency Raman scattering by Uchino and Yoko [73]. The temperature range in their study was somewhat higher but the peak was found situated at frequencies very close to the ones measured by THz-TDS as shown in Fig. 1(f). At 170 K, the intensity at frequencies below the frequency of the maximum is very similar. It is notable that while in the Raman data a distinct peak with a well-defined maximum was observed at 260 K, no distinct peak shape is obvious in the terahertz data.

Light scattering data acquired by Wuttke *et al.* [44] also show the BP located at approximately 1.5 THz at temperatures above 173 K. In their data, the BP does not disappear completely, even at elevated temperatures in the liquid regime. The agreement with terahertz data is good for low temperatures, as shown in Fig. 2.

It has been shown both experimentally and theoretically that the α relaxation observed in dielectric experiments is stronger than in scattering experiments [9,74,75]. This explains the differences observed between different experimental methods in Figs. 1(d) and 3(b).

While the BP itself is temperature independent [27,29,76], additional anharmonic effects that contribute to the absorption give the impression of an apparent shift of the BP with temperature. By tracking the changes of the apparent maximum we can observe when the anharmonic effects influence the absolute maximum intensity. This process ultimately results in the intensity of the BP being subsumed entirely by the anharmonic contributions to the absorption intensity.
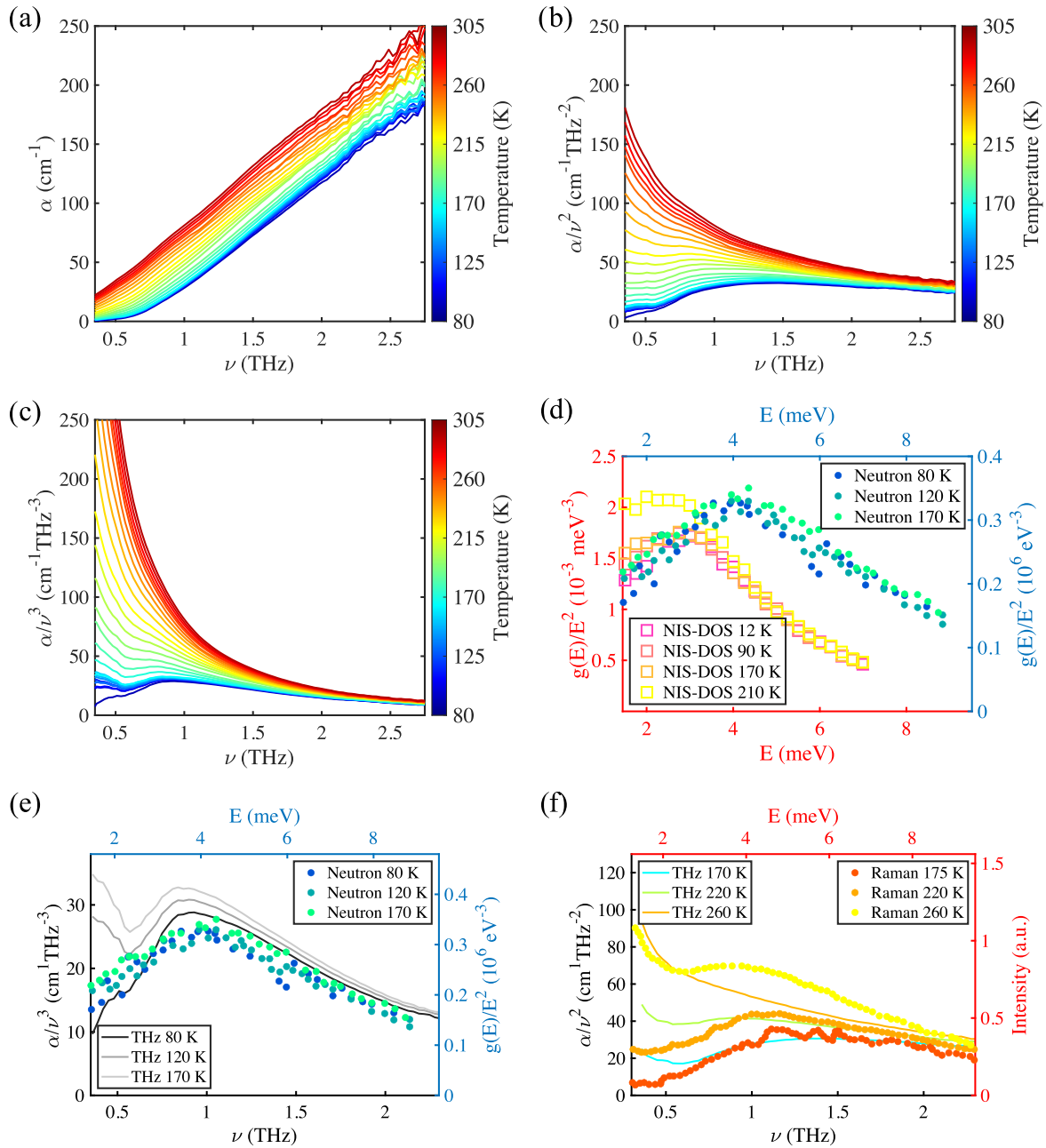
FIG. 1. Comparison of terahertz to neutron, nuclear inelastic scattering, and Raman data. (a) THz-TDS absorption spectrum of glycerol for temperature steps of 10 K from 80 to 280 K and steps of 5 K above. The sample is amorphous over the range of temperatures measured and absorption increases with temperature at all frequencies. [(b), (c)] BP visualized from the same data by plotting (b) α/ν^2 and (c) α/ν^3. A broad maximum is visible at around 1.3 THz at low temperatures that disappears upon heating. (d) Comparison of the BP in the VDOS measured with neutron scattering ([22], dots) and the BP measured with nuclear inelastic scattering ([24], squares). The latter maximum is located at slightly lower frequencies than in the neutron scattering data. (e) Comparison of the BP in the VDOS measured with neutron scattering ([22], dots) and α/ν^3 measured with THz-TDS (lines). The maxima and shapes are very similar. (f) Comparison of the α/ν^2 measured with THz-TDS (lines) and the VDOS measured with Raman scattering ([73], dots). The maxima below 260 K occur at similar frequencies and the shape is very similar.

To track the apparent change in the peak frequency (ν_{BP}) and its intensity, the data are first smoothed with a moving average and the numerical derivative is calculated. To determine whether the BP is still discernible at elevated temperatures, the inflection point in the density of states (DOS) is also calculated from the derivative and is shown in Fig. 3 for different temperatures. ν_{BP} and the inflection point are plotted

against temperature in Fig. 4. In pure glycerol, the decrease in the apparent center frequency of the BP is very sudden. For comparison, the more subtle change in some of the glycerol-water mixtures is shown in Supplemental Fig. S3 [63].

The behavior of the BP is hence described by a set of three parameters: the center frequency at the lowest measured temperature (approximately 0.9 THz), the temperature at which
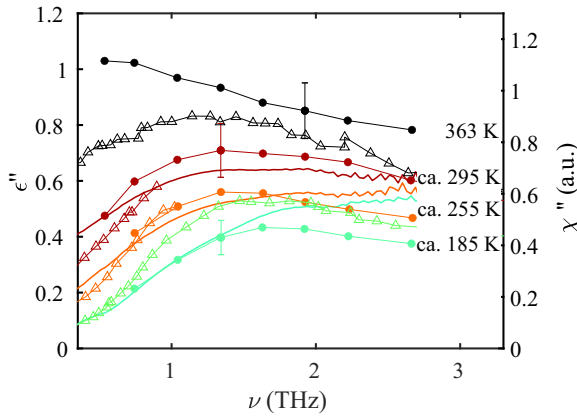
FIG. 2. Comparison of our spectra with light and neutron scattering relative permittivity and susceptibility. Solid lines correspond to the spectra measured in this work; the solid circles represent data from Schneider *et al.* [9], and triangles correspond to data from Wuttke *et al.* [44] (lines are plotted as a guide to the eye).

the center frequency is affected by anharmonic effects and appears to decrease (T^*, in glycerol approximately 170 K), and the highest temperature at which an inflection point is still present in the DOS (T_g^*, in glycerol 210 K, Fig. 4).

2. The absorption coefficient at cryogenic temperatures

The temperature behavior of glasses can be separated into three regimes. At low temperatures in the harmonic regime, any mobility (e.g., dihedral angle changes) is severely restricted and molecules vibrate at their equilibrium position due to their thermal energy. An increase in thermal energy results in an approximately linear increase in absorption that can be measured throughout the accessible frequency range. This also affects the apparent intensity of the (itself temperature-independent) BP. The onset of local mobility at T^* coincides with a transition region which is concluded by T_g^* and the anharmonic regime. With increasing temperature, the VDOS is further enhanced until the liquid state (the third regime) is reached, where quasielastic scattering occurs and makes it impossible to observe the BP.

The calorimetric glass transition temperature T_g of glycerol is hard to detect with THz-TDS, as has previously been reported by Sibik *et al.* [50] and Capaccioli *et al.* [77]. Sibik *et al.* [50] found a mean T_g^* of 194 K. Capaccioli *et al.* [77] argued that a secondary glass transition $T_{g,\beta}$ at 161 K was consistent with the same T_g^*. The T_g^* reported in the following is not the calorimetric glass transition temperature because our definition is not based directly on relaxation times but rather on what we observe with THz-TDS and hence expected to be different. We were interested in investigating what information we could gather with this technique instead.

When the spectra can be described by a linear function, the derivative (or slope) a also yields information about the strength of anharmonic processes.

The slope a is, in principle, a derivative and, as such, contains increased uncertainties. To increase the reliability of the data, we, therefore, selected a frequency range where the absorption coefficient is approximately linear so we can

calculate average slopes that are more accurate. The first derivative is plotted to determine the best-suited frequency ranges, as depicted in Fig. 5(a). This shows that the spectra can be approximated with linear functions below 0.5 THz and above 1.25 THz. These frequencies lie below and above the BP, respectively, and in these regions, the average slopes mirror the behavior of the ν_{BP}. Interestingly, lower frequencies are more strongly influenced by T^* and higher frequencies by T_g^*.

Below T^*, the slopes a at low frequencies are almost constant, implying that anharmonic effects do not dominate [Fig. 5(b)]. Above T^*, however, a increases noticeably. The slope at higher frequencies is temperature dependent even below T^*. At T_g^*, a jump is observed, and a decreases, as shown in Fig. 5(b).

Previous dielectric spectroscopy and neutron scattering experiments covering a more comprehensive frequency range have identified the MCT fast process at low temperatures and the structural α relaxation at higher temperatures as a source of the observed intensity shifts [9,44]. Our interpretation is consistent with MCT and their predictions.

These observations and explanations are now used to examine the influence of water content and temperature on the behavior of glycerol-water mixtures.

B. The influence of water concentration and temperature on glycerol-water mixtures

When data at various concentrations are reported, one has to keep in mind that Starciuc *et al.* showed that the transition from predominantly unclustered water molecules to clusters occurs at around 6.1 ± 0.7 wt % water. A second threshold was found at 18.6 ± 4.4 wt % water and linked to larger, percolating water clusters [57]. At concentrations below the first threshold, water molecules are predominantly unclustered, do not induce major structural changes, and form mostly water-glycerol hydrogen bonds. The LLT found by Murata and Tanaka occurs at higher water concentrations than investigated here [58]. Any change in behavior found at approximately 6 or 19 wt % water can therefore be attributed to the influence of water on the structural dynamics by increasing the cluster size and connectivity, as well as a strengthening of the hydrogen bonds between water molecules.

1. Harmonic regime ($T \leqslant T_g^*$)

The BP is shown for all samples in Fig. 6(a) at a temperature of 90 K. The dependence of its center frequency and intensity on water content are shown in Fig. 6(b). In most measurements, the BP is centered at 0.95 THz. In measurements where the BP is less pronounced, the center frequency deviates from that value. This seems to be more likely at water concentrations below 5 wt %.

In the harmonic regime, unclustered and clustered water molecules do not influence the center frequency of the BP. The Ioffe-Regel crossover is linked to the center frequency of the BP and denotes a crossover from wavelike to random-matrix-like physics as the mean free path of transverse waves becomes equal to their wavelength [24,29,76]. The results indicate that the Ioffe-Regel crossover is not influenced by the presence of clustered or unclustered water.
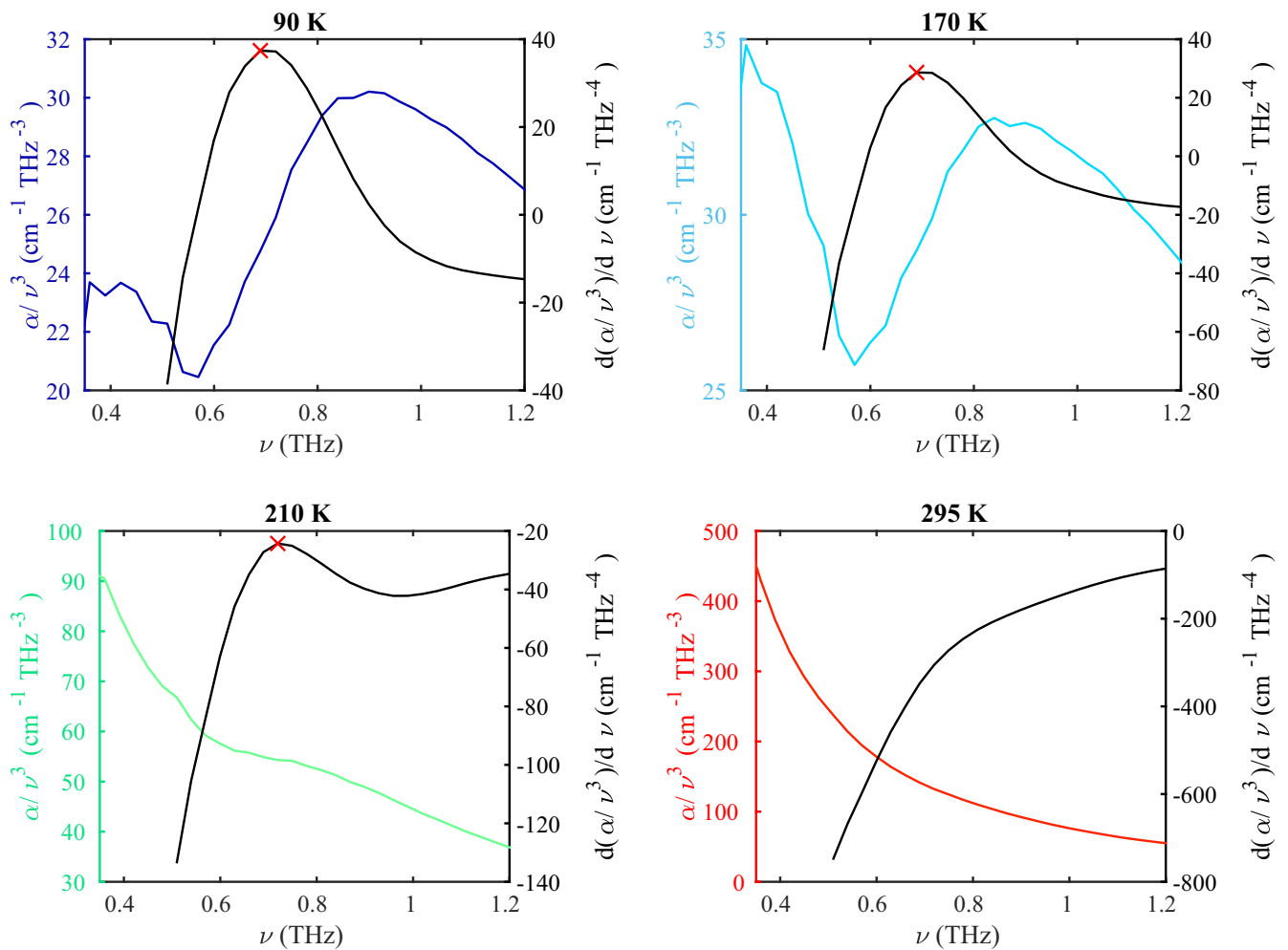
FIG. 3. The density of states and its derivative for different temperatures. The inflection point is highlighted with a cross in the derivative. At 295 K, the BP is obscured by anharmonic effects and neither an inflection point nor a maximum in the DOS can be found.
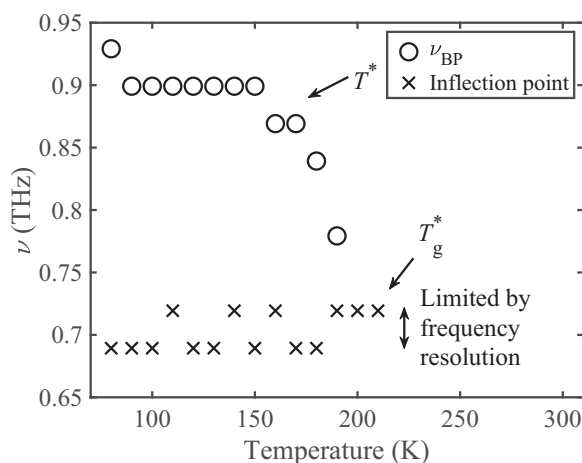

FIG. 4. ν_{BP} (circles) and inflection point (crosses) for glycerol for different temperatures as determined from smoothed data. Above 210 K, no inflection points and maxima were found. The frequency resolution (approximately 30 GHz) in the smoothed data limits the accuracy when determining T^* and T_g^*.

The onset of water clustering may decrease the intensity of the BP slightly, indicating a higher level of disorder. While the center frequency is largely independent of water content, the peak intensity may exhibit a shallow minimum around a concentration of about 5 wt % [as shown in Fig. 6(b)] when water molecules are homogeneously distributed throughout the sample.

In Fig. 7(a), an overview of the different transition temperatures is given for all glycerol-water mixtures measured for transition temperatures based on the different methods introduced when discussing pure glycerol. The temperatures at which the BP appears to shift and dissolves are characterized for all samples and the results are also shown in Fig. 7 together with the transition temperatures that are extracted from the anharmonicity parameter a in low- and high-frequency bands.

For clarity, the different T^* have been combined into a mean T^*, shown in Fig. 7(b), and can be interpreted to have only a weak dependence on water content below approximately 5wt.%, if any, and decreases at higher concentrations.

This means that unclustered water molecules do not change the temperature at which anharmonic effects result in an
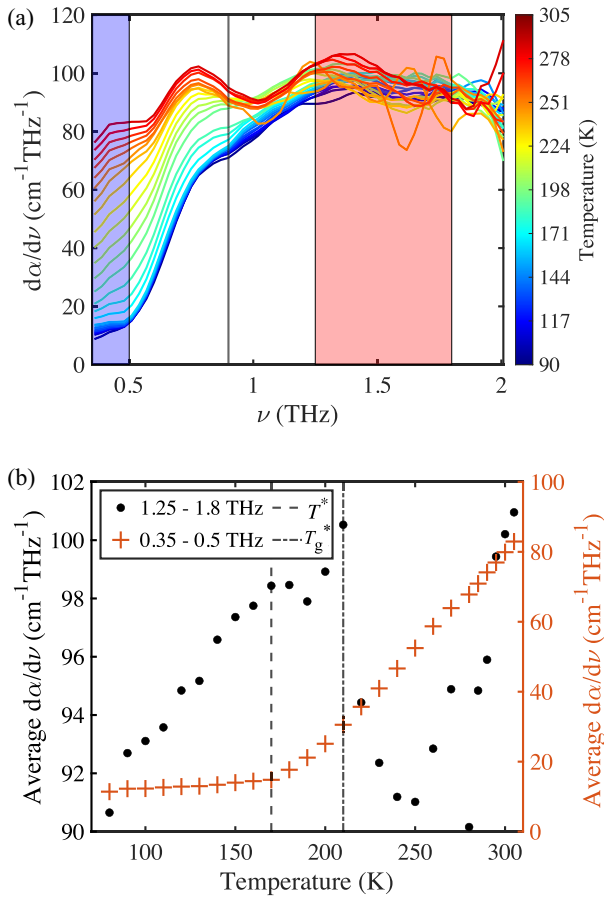
FIG. 5. (a) First derivative of spectra. Above approximately 1.25 THz and below 0.5 THz, the spectra can be described by linear functions. The vertical line denotes ν_{BP}. (b) Temperature dependence of average gradient for frequencies between 1.25 and 1.8 THz (dots) and 0.35 and 0.5 THz (crosses), i.e., the anharmonicity parameter a. Shown by vertical lines are also T^* and T_g^*.
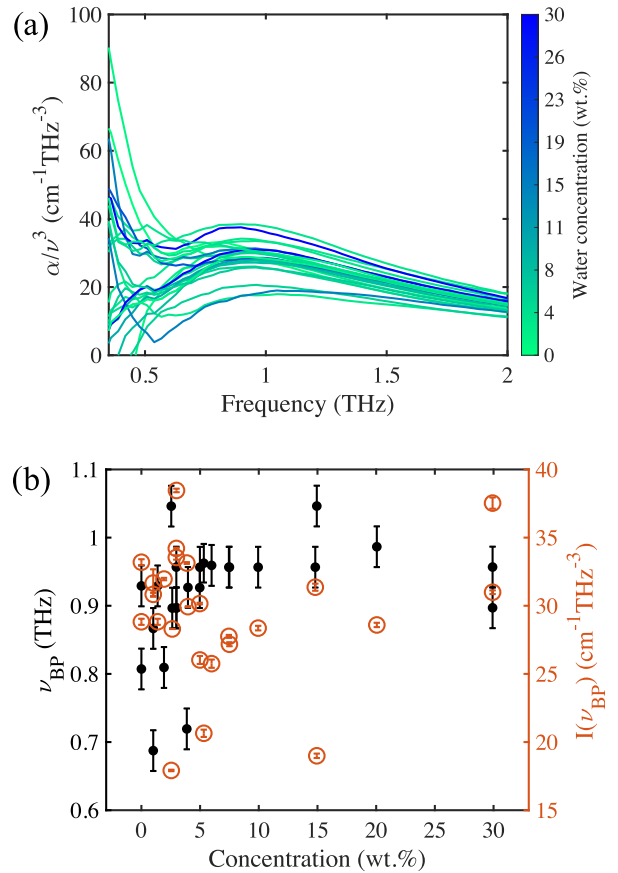

FIG. 6. (a) BP at 90 K for all samples. (b) Center frequency (black dots) and intensity (orange circles) at 90 K for all measured water concentrations.

apparent shift of the BP. The height of the energy barrier separating the harmonic from the anharmonic regime is hence not influenced by unclustered water molecules embedded in the glycerol matrix.

The shape of the deepest minimum of the PES is independent of water concentration or the presence of water clusters, as otherwise the rate of change of the anharmonicity parameter a would be different, as shown in Fig. 7(c). A change in a with temperature corresponds to increased anharmonic contributions.

At water concentrations above 5 wt %, parameters change their behavior: the intensity of the BP increases slightly with concentration (Fig. 6), and anharmonic effects decrease the temperature at which they influence the appearance of the BP (Fig. 7).

A neutron scattering study by Towey *et al.* [59–61] has shown that at a concentration of 5 wt %, water monomers are distributed homogenously throughout the material. As the water concentration is increased, water clusters coexist with unclustered water molecules. Past studies suggest that the onset of mobility in amorphous water may lie in the range -137 deg C to -149 deg C [78–81] and the PES of bulklike

water is hence expected to comprise shallower minima than that of glycerol where the onset of mobility lies at higher temperatures. The THz-TDS results indicate a shift in the structural dynamics once clusters form, accompanied by a reduced height of the potential energy barrier separating the harmonic from the anharmonic regime.

As the water concentration is increased up to 16.4 wt % water, the percentage of water molecules that are part of clusters increases to 80% [59–61]. In our THz-TDS measurements we do not see a difference between T^* for mixtures containing 15 and 20 wt %. This indicates that the presence of water-water hydrogen bonds lowers the barriers on the PES, but, once clusters dominate, the intensity of anharmonic effects does not depend on the number of clusters, but on their mean size.

Water-water cooperative domains [82,83] and percolating water clusters [57] have been found at even higher water content. In our THz-TDS measurements, the onset temperature of anharmonic effects is decreased noticeably in samples with a water concentration of 30 *wt* % as shown in Fig. 7(b). We can hence infer that the mean size of clusters influences the PES and thereby structural dynamics stronger than their number and that the height of the lowest energy barrier is the limiting factor determining the onset temperature of anharmonicity. Regions with lower energy barriers first exhibit an increase in mobility which is measured by THz-TDS.
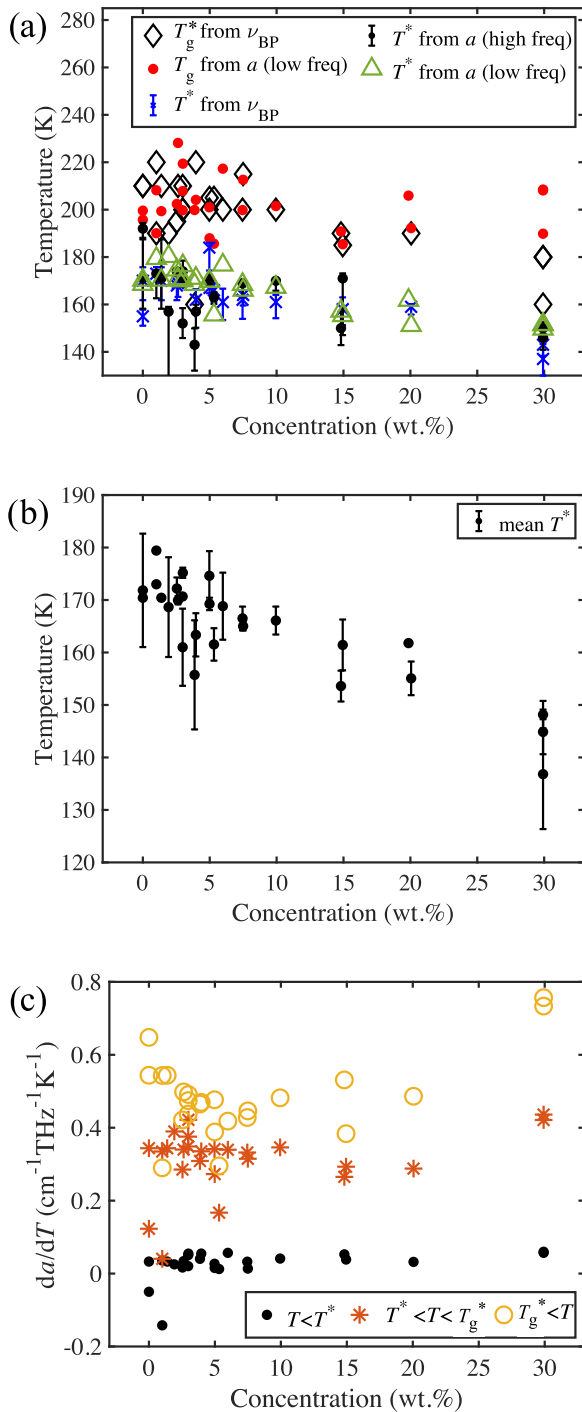
FIG. 7. (a) Different transition temperatures characterizing the onset of mobility and anharmonicity and the temperature at which the BP dissolves. (b) Mean T^* for different water contents. (c) Rate of change of the anharmonicity parameter at frequencies below the boson peak [see Fig. 5(b)], with temperature in different temperature regimes. Above T_g^*, a shallow minimum is observed around 5 wt %.

2. Anharmonic regime ($T_g^* < T < T_m$)

Below T^*, the rate of absorption change does not strongly depend on water content, as shown in Fig. 7(c). Above T_g^*, the rate of absorption change starts to increase with water concentration above 5 wt % water [see Fig. 7(c)]. There is

also evidence for a shallow minimum at around 5 wt % which could be due to a very homogenous sample including many unclustered water molecules.

Unclustered water reduces the rate of change of the anharmonicity parameter at a water content below 30 *wt* % compared to pure glycerol. This "plasticizer effect" could be because the unclustered water molecules are surrounded by larger glycerol molecules, and any reorientation of the glycerol molecules first requires the breaking of hydrogen bonds with water. Once clusters are formed, however, the larger mobility of water molecules in a bulklike environment increases the rate again.

The higher the temperature and mobility, the more anharmonic effects obscure the BP until it can no longer be resolved. T_g^* as defined in Fig. 5(b) does not depend on water content below 10 wt %, and decreases for water concentrations up to 30 wt %. This indicates that the presence of a number of larger water clusters increases anharmonic effects. Unclustered water and small isolated clusters have no effect.

Raman scattering experiments have shown that an underlying BP continues to be present above T_g [73] which can no longer be resolved by THz-TDS because it is obscured by anharmonic effects.

The calorimetric T_g as measured with DSC shows a dependence on water concentration even below 10 wt % [57]. This can be attributed to the different criteria for determining the exact value. While the calorimetric T_g is related to a change in heat flow, our definition of T_g^* based on anharmonic effects is therefore expected to result in slightly different values.

Upon further heating the supercooled liquid, it enters the liquid regime.

3. Liquid regime ($T = 293$ K)

A room-temperature (293 K) setup was utilized to measure glycerol-water mixtures in the same concentration range (0–30 wt % water) as discussed above. With this setup it was easy to repeat measurements very rapidly and the spectra shown in Fig. S5(a) are the average of 18 measurements each [63]. The absolute error associated with the absorption coefficient measurement is hence decreased and the data quality and spectral range are better than for measurements performed at variable temperatures.

At room temperature, the mixtures are fully liquid and no BP can be detected. The absorption coefficient at 1 THz depends linearly on water concentration c, as can be seen in Fig. S5(b) of the Supplemental Material [63]:

$$\alpha(c) = 1.47 \, \text{cm}^{-1}\%^{-1} \times c[\text{wt}\%] + 65.6 \, \text{cm}^{-1} \qquad (12)$$

and the presence or absence of water clusters does not seem to influence this relationship. To investigate how water clusters influence the THz-TDS spectra of liquid glycerol-water mixtures, the frequency-dependent absorption is hence evaluated.

Chumakov *et al.* provided a phenomenological description of the spectral shape of the reduced density of states found at frequencies beyond ν_{BP} in glycerol and other studied glasses [24]:

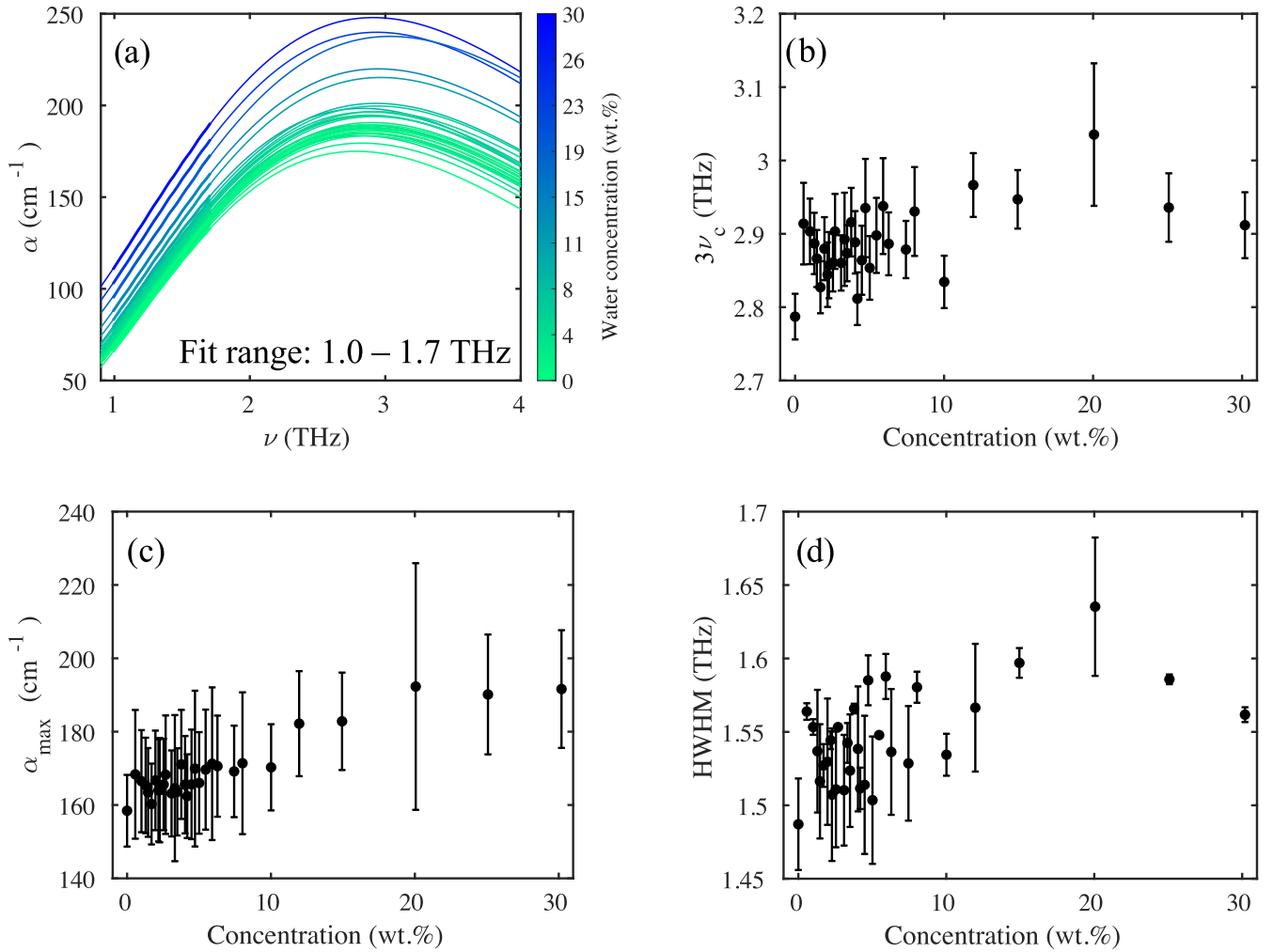$$\frac{g(E)}{E^2} \propto \exp\left(\frac{-E}{E_0}\right). \qquad (13)$$

FIG. 8. (a) Measured spectra (up to 2.5 THz) and extrapolated spectra at higher frequencies. (b) Predicted center frequency, (c) maximum absorption, and (d) half width at half maximum of the spectral shape for different water contents. Error bars are calculated from 95% confidence interval of the fit.

We can now relate this expression to the measured IR absorption coefficient according to Eq. (11):

$$\frac{\alpha(w)}{\omega^3} \propto \exp\left(\frac{-\omega}{\omega_0}\right). \tag{14}$$

The observations of Chumakov *et al.* were restricted to the frequency range 4–7 meV, i.e., approximately 1–1.7 THz. We hence fit the function

$$\alpha = A\nu^3 \exp\left(-\nu/(\nu_c)\right) + C \tag{15}$$

to the measured absorption coefficient in the same range, as shown in Fig. 8(a). The results for different upper fit limits are shown in the supporting information; however, these limits do not fundamentally affect the features discussed in the following. The fit function exhibits a maximum at $3\nu_c$. To characterize the function, we examine the dependence of fit parameter ν_c on concentration, as shown in Fig. 8(b). Further characteristics of the fit functions are its maximum α_{max} and the half width at half maximum (HWHM). Measured spectral

data are reduced to the fit parameters and the influence of water concentration is examined.

As expected, an increase in water content leads to an increase in absorption, as well as to a broadening of the peak. This also leads to the previously discussed increase in the absorption at 1 THz.

Unclustered water molecules are tightly integrated into the hydrogen network, with most glycerol hydrogen bonds formed between water and glycerol molecules [57]. Above the glass transition temperature, these water molecules exhibit different degrees of freedom which broaden the spectral feature at higher frequencies. Increasing the amount of unclustered water leads to the most noticeable change in those three parameters over the whole concentration range studied.

At concentrations below 6 *wt* %, the maximum absorption is mainly independent of water content. Once water clusters form, the number of water-glycerol hydrogen bonds decreases and the number of water-water bonds increases. Once clusters are present, a higher water content increases the cluster size. Within the clusters, the water dynamics are markedly different from unclustered water molecules that are hydrogen-bonded to glycerol.

While the second clustering threshold just below 20 *wt %* was not clearly observed in the BP, it influences the behavior of the system at higher frequencies. All three parameters describing the VDOS change less above a water content of 20 *wt %*. Most notably, the center frequency decreases above 20 *wt %*. At room temperature, bulk water has a higher absorption at 1 THz than glycerol ($220 \, \mathrm{cm}^{-1}$ compared to $66 \, \mathrm{cm}^{-1}$) and the larger the water clusters, the more they behave like bulk water. Once percolating water clusters form, they dominate the absorption of liquid glycerol-water mixtures at higher frequencies comprising the VDOS.

IV. CONCLUSIONS

While the terahertz spectra of amorphous solids and liquids are featureless, they provide considerable information about glass transition temperatures and the related mobility changes. They also offer insight into the vibrational density of states and the BP.

We show that the infrared absorption coefficient measured with THz-TDS can be theoretically related to the reduced Raman intensity ($\propto \alpha/\omega^2$) and the reduced DOS ($\propto \alpha/\omega^3$) and the agreement with experimental results confirms this.

The temperature behavior is characterized by three regimes: Below the glass transition temperature, the system is trapped in a deep minimum of the potential energy landscape and exhibits mostly harmonic vibrations. The onset of local and (at slightly higher temperatures) global mobility is accompanied by anharmonic excitations, obscuring the BP and eventually leading to its dissolution. Once the system crosses over into the liquid regime, the absorption spectra are dominated by quasielastic scattering.

The implications are examined in detail on the example of glycerol and the insights are applied to study the influence of clustered and unclustered water.

In the harmonic regime, the shape of the PES is unaltered in the presence of clustered and unclustered water molecules. Unclustered water molecules are embedded into the glycerol matrix and do not decrease the onset temperature of anharmonicity. A change in structural dynamics is observed at a water concentration of approximately 5 wt %, corresponding to a transition from isolated water molecules distributed homogeneously throughout the sample to the presence of small water clusters and an increased number of water-water hydrogen bonds which lower the barriers on the PES.

Interestingly, the intensity of anharmonic effects does not depend on the number of water clusters but on their mean size.

Data acquired at room temperature are extrapolated according to a model by Chumakov *et al.* which allows to investigate the spectral shape for different concentrations for liquid glycerol-water mixtures and confirms a change of dynamics once percolating water clusters formed between 15 and 20 wt %.

This methodology has great potential to be applied to other systems to investigate the change of mobility and dynamics.

[1] C. Corsaro, E. Fazio, and D. Mallamace, The Stokes-Einstein relation in water/methanol solutions, J. Chem. Phys. **150**, 234506 (2019).

[2] V. Lubchenko and P. G. Wolynes, Theory of structural glasses and supercooled liquids, Annu. Rev. Phys. Chem. **58**, 235 (2007).

[3] A. Cavagna, Supercooled liquids for pedestrians, Phys. Rep. **476**, 51 (2009).

[4] W. Götze, The essentials of the mode-coupling theory for glassy dynamics, Condens. Matter Phys. **1**, 873 (1998).

[5] W. Götze, *Complex Dynamics of Glass-Forming Liquids: A Mode-Coupling Theory*, Vol. 143 (Oxford University Press, 2009).

[6] M. Goldstein, Viscous liquids and the glass transition: A potential energy barrier picture, J. Chem. Phys. **51**, 3728 (1969).

[7] A. Meyer, J. Wuttke, W. Petry, A. Peker, R. Bormann, G. Coddens, L. Kranich, O. G. Randl, and H. Schober, Harmonic behavior of metallic glasses up to the metastable melt, Phys. Rev. B **53**, 12107 (1996).

[8] P. Lunkenheimer, A. Pimenov, M. Dressel, Y. G. Goncharov, R. Böhmer, and A. Loidl, Fast Dynamics of Glass-Forming Glycerol Studied by Dielectric Spectroscopy, Phys. Rev. Lett. **77**, 318 (1996).

[9] U. Schneider, P. Lunkenheimer, R. Brand, and A. Loidl, Dielectric and far-infrared spectroscopy of glycerol, J. Non-Cryst. Solids **235–237**, 173 (1998).

[10] N. Menon, K. P. O'Brien, P. K. Dixon, L. Wu, S. R. Nagel, B. D. Williams, and J. P. Carini, Wide-frequency dielectric susceptibility measurements in glycerol, J. Non-Cryst. Solids **141**, 61 (1992).

[11] E. Rössler, A. P. Sokolov, A. Kisliuk, and D. Quitmann, Low-frequency raman scattering on different types of glass formers used to test predictions of mode-coupling theory, Phys. Rev. B **49**, 14967 (1994).

[12] P. Lunkenheimer, R. Wehn, T. Riegger, and A. Loidl, Excess wing in the dielectric loss of glass formers: Further evidence for a β-relaxation, J. Non-Cryst. Solids **307–310**, 336 (2002).

[13] P. G. Debenedetti and F. H. Stillinger, Supercooled liquids and the glass transition, Nature (London) **410**, 259 (2001).

[14] G. P. Johari and M. Goldstein, Viscous liquids and the glass transition. II. Secondary relaxations in glasses of rigid molecules, J. Chem. Phys. **53**, 2372 (1970).

[15] G. P. Johari, Intrinsic mobility of molecular glasses, J. Chem. Phys. **58**, 1766 (1973).

[16] Y. Yomogida, Y. Sato, R. Nozaki, T. Mishina, and J. Nakahara, Comparative dielectric study of monohydric alcohols with

terahertz time-domain spectroscopy, J. Mol. Struct. **981**, 173 (2010).

[17] Y. Yomogida, Y. Sato, R. Nozaki, T. Mishina, and J. Nakahara, Comparative study of boson peak in normal and secondary alcohols with terahertz time-domain spectroscopy, Phys. B: Condens. Matter **405**, 2208 (2010).

[18] Y. Yomogida, Y. Sato, K. Yamakawa, R. Nozaki, T. Mishina, and J. Nakahara, Comparative dielectric study of pentanol isomers with terahertz time-domain spectroscopy, J. Mol. Struct. **970**, 171 (2010).

[19] J. P. Poley, Microwave dispersion of some polar liquids, Appl. Sci. Res. **4**, 337 (1955).

[20] G. Johari, Molecular inertial effects in liquids: Poley absorption, collision-induced absorption, low-frequency Raman spectrum and boson peaks, J. Non-Cryst. Solids **307–310**, 114 (2002).

[21] U. Buchenau, N. Nücker, and A. J. Dianoux, Neutron Scattering Study of the Low-Frequency Vibrations in Vitreous Silica, Phys. Rev. Lett. **53**, 2316 (1984).

[22] J. Wuttke, W. Petry, and S. Pouget, Structural relaxation in viscous glycerol: Coherent neutron scattering, J. Chem. Phys. **105**, 5177 (1996).

[23] V. M. Giordano and G. Monaco, Inelastic x-ray scattering study of liquid Ga: Implications for the short-range order, Phys. Rev. B **84**, 052201 (2011).

[24] A. I. Chumakov, I. Sergueev, U. van Buerck, W. Schirmacher, T. Asthalter, R. Rüffer, O. Leupold, and W. Petry, Collective Nature of the Boson Peak and Universal Transboson Dynamics of Glasses, Phys. Rev. Lett. **92**, 245508 (2004).

[25] Z. Pan, O. Benzine, S. Sawamura, R. Limbach, A. Koike, T. D. Bennett, G. Wilde, W. Schirmacher, and L. Wondraczek, Disorder classification of the vibrational spectra of modern glasses, Phys. Rev. B **104**, 134106 (2021).

[26] P. Lunkenheimer and A. Loidl, High-frequency excitations in glassy crystals, J. Non-Cryst. Solids **352**, 4556 (2006).

[27] W. Schirmacher, G. Diezemann, and C. Ganter, Harmonic Vibrational Excitations in Disordered Solids and the "Boson Peak", Phys. Rev. Lett. **81**, 136 (1998).

[28] W. Schirmacher, Thermal conductivity of glassy materials and the boson peak, Europhys. Lett. **73**, 892 (2006).

[29] W. Schirmacher, T. Scopigno, and G. Ruocco, Theory of vibrational anomalies in glasses, J. Non-Cryst. Solids **407**, 133 (2015).

[30] A. Marruzzo, W. Schirmacher, A. Fratalocchi, and G. Ruocco, Heterogeneous shear elasticity of glasses: The origin of the boson peak, Sci. Rep. **3**, 1407 (2013).

[31] S. N. Taraskin, S. I. Simdyankin, S. R. Elliott, J. R. Neilson, and T. Lo, Universal Features of Terahertz Absorption in Disordered Materials, Phys. Rev. Lett. **97**, 055504 (2006).

[32] A. I. Chumakov, G. Monaco, A. Monaco, W. A. Crichton, A. Bosak, R. Rüffer, A. Meyer, F. Kargl, L. Comez, D. Fioretto, H. Giefers, S. Roitsch, G. Wortmann, M. H. Manghnani, A. Hushur, Q. Williams, J. Balogh, K. Parlinski, P. Jochym, and P. Piekarz, Equivalence of the Boson Peak in Glasses to the Transverse Acoustic van Hove Singularity in Crystals, Phys. Rev. Lett. **106**, 225501 (2011).

[33] A. I. Chumakov, G. Monaco, A. Fontana, A. Bosak, R. P. Hermann, D. Bessas, B. Wehinger, W. A. Crichton, M. Krisch, R. Rüffer *et al.*, Role of Disorder in the Thermodynamics and

Atomic Dynamics of Glasses, Phys. Rev. Lett. **112**, 025502 (2014).

[34] V. Karpov, I. Klinger, and F. Ignat'Ev, Theory of the low-temperature anomalies in the thermal properties of amorphous structures, Zh. Eksp. Teor. Fiz **84**, 775 (1983).

[35] E. Lerner and E. Bouchbinder, Low-energy quasilocalized excitations in structural glasses, J. Chem. Phys. **155**, 200901 (2021).

[36] U. Buchenau, Y. M. Galperin, V. L. Gurevich, D. A. Parshin, M. A. Ramos, and H. Schober, Interaction of soft modes and sound waves in glasses, Phys. Rev. B **46**, 2798 (1992).

[37] V. Gurarie and J. T. Chalker, Bosonic excitations in random media, Phys. Rev. B **68**, 134207 (2003).

[38] C. Wang and R. Wright, Raman scattering studies of liquids and glasses. I. Liquid and supercooled liquid glycerol, J. Chem. Phys. **55**, 1617 (1971).

[39] C. Wang and R. Wright, Raman scattering studies in liquids and glasses. II. Liquid and supercooled liquid glycerol, J. Chem. Phys. **55**, 3300 (1971).

[40] J. L. Dashnau, N. V. Nucci, K. A. Sharp, and J. M. Vanderkooi, Hydrogen bonding and the cryoprotective properties of glycerol/water mixtures, J. Phys. Chem. B **110**, 13670 (2006).

[41] T. Perova, D. Christensen, U. Rasmussen, J. Vij, and O. Nielsen, Far-infrared spectra of highly viscous liquids: Glycerol and triacetin (glycerol triacetate), Vib. Spectrosc. **18**, 149 (1998).

[42] S. Murthy, Experimental study of the dynamics of water and the phase behavior of the supercooled aqueous solutions of propylene glycol, glycerol, poly(ethylene glycol)s, and poly(vinylpyrrolidone), J. Phys. Chem. B **104**, 6955 (2000).

[43] J. Huck, G. Noyel, and L. Jorat, Dielectric properties of supercooled glycerol-water solutions, IEEE Trans. Electr. Insul. **23**, 627 (1988).

[44] J. Wuttke, J. Hernandez, G. Li, G. Coddens, H. Z. Cummins, F. Fujara, W. Petry, and H. Sillescu, Neutron and Light Scattering Study of Supercooled Glycerol, Phys. Rev. Lett. **72**, 3052 (1994).

[45] T. E. Dirama, G. A. Carri, and A. P. Sokolov, Role of hydrogen bonds in the fast dynamics of binary glasses of trehalose and glycerol: A molecular dynamics simulation study, J. Chem. Phys. **122**, 114505 (2005).

[46] C. Angell and D. Smith, Test of the entropy basis of the Vogel-Tammann-Fulcher equation. Dielectric relaxation of polyalcohols near T_g, J. Phys. Chem. **86**, 3845 (1982).

[47] J. Sibik and J. A. Zeitler, Terahertz spectroscopy of hydrogen-bonded glass-forming liquids, in *2013 38th International Conference on Infrared, Millimeter, and Terahertz Waves (IRMMW-THz)* (IEEE, Piscataway, NJ, 2013), pp. 1–3.

[48] R. Busselez, R. Lefort, M. Guendouz, B. Frick, O. Merdrignac-Conanec, and D. Morineau, Molecular dynamics of glycerol and glycerol-trehalose bioprotectant solutions nanoconfined in porous silicon, J. Chem. Phys. **130**, 214502 (2009).

[49] Y. E. Ryabov, Y. Hayashi, A. Gutina, and Y. Feldman, Features of supercooled glycerol dynamics, Phys. Rev. B **67**, 132202 (2003).

[50] J. Sibik, S. R. Elliott, and J. A. Zeitler, Thermal decoupling of molecular-relaxation processes from the vibrational density of states at terahertz frequencies in supercooled hydrogen-bonded liquids, J. Phys. Chem. Lett. **5**, 1968 (2014).

[51] J. Wuttke, W. Petry, G. Coddens, and F. Fujara, Fast dynamics of glass-forming glycerol, Phys. Rev. E **52**, 4026 (1995).

[52] J. Sibik, K. Looebmann, T. Rades, and J. A. Zeitler, Predicting crystallization of amorphous drugs with terahertz spectroscopy, Mol. Pharm. **12**, 3062 (2015).

[53] M. T. Ruggiero, M. Krynski, E. O. Kissi, J. Sibik, D. Markl, N. Y. Tan, D. Arslanov, W. Van Der Zande, B. Redlich, T. M. Korter *et al.*, The significance of the amorphous potential energy landscape for dictating glassy dynamics and driving solid-state crystallisation, Phys. Chem. Chem. Phys. **19**, 30039 (2017).

[54] J. M. Sztein, T. Takeo, and N. Nakagata, History of cryobiology, with special emphasis in evolution of mouse sperm cryopreservation, Cryobiology **82**, 57 (2018).

[55] M. T. Cicerone, M. J. Pikal, and K. K. Qian, Stabilization of proteins in solid form, Adv. Drug Delivery Rev. **93**, 14 (2015).

[56] E. Y. Shalaev and G. Zografi, How does residual water affect the solid-state degradation of drugs in the amorphous state? J. Pharm. Sci. **85**, 1137 (1996).

[57] T. Starciuc, Y. Guinet, A. Hedoux, and E. Shalaev, Water content thresholds in glycerol/water system: Low- and high-wavenumber Raman spectroscopy study, J. Mol. Liq. **321**, 114678 (2021).

[58] K.-i. Murata and H. Tanaka, Liquid-liquid transition without macroscopic phase separation in a water-glycerol mixture, Nat. Mater. **11**, 436 (2012).

[59] J. Towey and L. Dougan, Structural examination of the impact of glycerol on water structure, J. Phys. Chem. B **116**, 1633 (2012).

[60] J. Towey, A. Soper, and L. Dougan, The structure of glycerol in the liquid state: A neutron diffraction study, Phys. Chem. Chem. Phys. **13**, 9397 (2011).

[61] J. Towey, A. Soper, and L. Dougan, Molecular insight into the hydrogen bonding and micro-segregation of a cryoprotectant molecule, J. Phys. Chem. B **116**, 13898 (2012).

[62] J. Sibik, E. Y. Shalaev, and J. A. Zeitler, Glassy dynamics of sorbitol solutions at terahertz frequencies, Phys. Chem. Chem. Phys. **15**, 11931 (2013).

[63] See Supplemental Material at http://link.aps.org/supplemental/10.1103/PhysRevB.107.104203 for BP center and inflection point frequencies plotted against temperature for mixtures, details of calculation of the absorption coefficient, and room-temperature spectra and absorption coefficient at 1 THz.

[64] L. Duvillaret, F. Garet, and J.-L. Coutaz, A reliable method for extraction of material parameters in terahertz time-domain spectroscopy, IEEE J. Sel. Top. Quantum Electron. **2**, 739 (1996).

[65] T. A. Shmool and J. A. Zeitler, Insights into the structural dynamics of poly lactic-*co*-glycolic acid at terahertz frequencies, Polym. Chem. **10**, 351 (2019).

[66] E. A. DiMarzio and M. Bishop, Connection between the macroscopic electric and mechanical susceptibilities, J. Chem. Phys. **60**, 3802 (1974).

[67] A. Gemant, The conception of a complex viscosity and its application to dielectrics, Trans. Faraday Soc. **31**, 1582 (1935).

[68] B. Jakobsen, K. Niss, and N. B. Olsen, Dielectric and shear mechanical alpha and beta relaxations in seven glass-forming liquids, J. Chem. Phys. **123**, 234511 (2005).

[69] W. Schirmacher, G. Ruocco, and V. Mazzone, Theory of heterogeneous viscoelasticity, Philos. Mag. **96**, 620 (2016).

[70] A. Martin and W. Brenig, Model for Brillouin scattering in amorphous solids, Phys. Status Solidi B **64**, 163 (1974).

[71] B. Schmid and W. Schirmacher, Raman Scattering and the Low-Frequency Vibrational Spectrum of Glasses, Phys. Rev. Lett. **100**, 137402 (2008).

[72] N. V. Surovtsev and A. P. Sokolov, Frequency behavior of Raman coupling coefficient in glasses, Phys. Rev. B **66**, 054205 (2002).

[73] T. Uchino and T. Yoko, Low-frequency Raman scattering and the fast relaxation process in glycerol, Science **273**, 480 (1996).

[74] N. Petzold, B. Schmidtke, R. Kahlau, D. Bock, R. Meier, B. Micko, D. Kruk, and E. Rössler, Evolution of the dynamic susceptibility in molecular glass formers: Results from light scattering, dielectric spectroscopy, and NMR, J. Chem. Phys. **138**, 12A510 (2013).

[75] M. Lebon, C. Dreyfus, Y. Guissani, R. Pick, and H. Cummins, Light scattering and dielectric susceptibility spectra of glass-forming liquids, Z. Phys. B **103**, 433 (1997).

[76] A. Marruzzo, S. Koehler, A. Fratalocchi, G. Ruocco, and W. Schirmacher, Vibrational anomalies and marginal stability of glasses, Eur. Phys. J.: Spec. Top. **216**, 83 (2013).

[77] S. Capaccioli, K. Ngai, M. S. Thayyil, and D. Prevosto, Coupling of caged molecule dynamics to JG β-relaxation: I, J. Phys. Chem. B **119**, 8800 (2015).

[78] G. Johari, A. Hallbrucker, and E. Mayer, The glass-liquid transition of hyperquenched water, Nature (London) **330**, 552 (1987).

[79] M. Sugisaki, H. Suga, and S. Seki, Calorimetric study of the glassy state. IV. Heat capacities of glassy water and cubic ice, Bull. Chem. Soc. Jpn. **41**, 2591 (1968).

[80] Y. Handa and D. Klug, Heat capacity and glass transition behavior of amorphous ice, J. Phys. Chem. **92**, 3323 (1988).

[81] E. Mayer, Calorimetric glass transitions in the amorphous forms of water: A comparison, J. Mol. Struct. **250**, 403 (1991).

[82] Y. Hayashi, A. Puzenko, and Y. Feldman, Slow and fast dynamics in glycerol-water mixtures, J. Non-Cryst. Solids **352**, 4696 (2006).

[83] S. Sudo, M. Shimomura, N. Shinyashiki, and S. Yagihara, Broadband dielectric study of $\alpha - \beta$ separation for supercooled glycerol–water mixtures, J. Non-Cryst. Solids **307–310**, 356 (2002).